Periodic DFT Study of the Structural and Electronic Properties of Bulk CoAl 2 O 4 Spinel

ARTICLE *in* THE JOURNAL OF PHYSICAL CHEMISTRY B · FEBRUARY 2006

Impact Factor: 3.3 · DOI: 10.1021/jp053375l · Source: PubMed

Periodic DFT Study of the Structural and Electronic Properties of Bulk $CoAl_2O_4$ Spinel

F. Tielens,*,† M. Calatayud,† R. Franco,‡ J. M. Recio,‡ J. Pérez-Ramírez,§ and C. Minot†

Laboratoire de Chimie Théorique, Université Pierre et Marie Curie, Paris VI, Case 137, 4 Place Jussieu, F-75252 Paris Cedex 05, France, Departamento de Química, Física y Analítica, Universidad de Oviedo, E-33006 Oviedo, Spain, and Laboratory for Heterogeneous Catalysis, Catalan Institution of Research and Advanced Studies (ICREA) and Institute of Chemical Research of Catalonia (ICIQ), Avenue Països Catalans s/n, E-43007 Tarragona, Spain

Received: June 22, 2005; In Final Form: November 4, 2005

In this study, structural and electronic properties of $CoAl_2O_4$ spinel are investigated for the first time by means of quantum chemical computational tools. Coupling supercell periodic calculations under the density functional theory formalism with a nonempirical quasi-harmonic Debye model, we examine the influence of temperature on the relative stability of several cation distributions of Co^{2+} and Al^{3+} over tetrahedral and octahedral interstices of the oxygen sublattice. Our simulations are able to reproduce the experimentally observed trend: (i) the normal spinel is calculated to be the stable structure at static and low-temperature conditions, and (ii) as the temperature increases, the preference of structures with Al^{3+} at tetrahedral sites (and Co^{2+} at octahedral sites) is found to progress following an asymptotic conduct. The effects of the cation distributions on geometrical variations of electronic and magnetic properties of $CoAl_2O_4$ can be interpreted as dominated by the local behavior of Co^{2+} at octahedral sites.

Introduction

The spinels AB_2X_4 constitute one of the most interesting and important families of crystalline compounds, with applications in many different areas as magnetic materials, ceramics, and catalysis.[1] In the stoichiometric formula AB_2X_4, equivalent to $(AX)(B_2X_3)$, the A indicates a divalent cation, B a trivalent cation, and X a divalent anion. Different compounds have this structure, mainly oxides and sulfides but also selenides and tellurides.[2−4] The A and B cations can occupy two different sites in the structure, octahedral (O_h) and tetrahedral (T_d). Studies of cation distributions in spinels are of considerable interest in solid-state chemistry for a better understanding of correlation between structure and properties such as color, diffusivity, magnetic behavior, conductivity, and catalytic activity etc., which are well-known to be dependent on the relative O_h and T_d occupancy by metals.[5−7]

The cation distribution of A and B cations over tetrahedral and octahedral sites in spinels is affected by the combination and nature of the two cations and depends strongly on pressure and temperature. The cation distribution can be unequivocally characterized by the so-called degree of inversion *x*. This parameter is defined as the fraction of the divalent metal cations in octahedral sites

$$(Co_{1-x}\,Al_x)[Co_xAl_{2-x}]O_4 \qquad (1)$$

In this formula, the parentheses and square brackets denote the tetrahedral and octahedral surroundings, respectively. Normal spinels have $x = 0$, while inverse spinels ($x = 1$) are found with divalent cations occupying octahedral sites and trivalent ones occupying tetrahedral and octahedral sites in equal proportion. When the degree of inversion is equal to 2/3, the spinel is called random since the di- and trivalent cations are randomly distributed among both coordinations, the number of trivalent cations being double than that of divalent cations in both tetrahedral and octahedral sites.

Typical normal spinels at room conditions are $MgAl_2O_4$, $FeAl_2O_4$, $ZnAl_2O_4$, and $FeCr_2O_4$, and typical inverse spinels are Fe_3O_4, $MgFe_2O_4$, and $MnFe_2O_4$.[8] Although it is possible to find in nature and to synthesize spinels in a more or less wide range of cation distributions, forcing normal spinels to be inverse is sometimes experimentally difficult or even impossible. Temperature has been the variable most widely used in this respect. Usually, an increasing of temperature yields to a continuous increase of the degree of inversion parameter. Sometimes a sudden finite change of *x* appears in a narrow range of temperature that is associated with an order−disorder phase transition of a second-order type, the prototypical $MgAl_2O_4$ spinel being one of the best examples showing this behavior.[9]

In this paper, we focus on the $CoAl_2O_4$ spinel. This spinel is also known as Thenard's (Dresden) blue and has been extensively used since 1802 as pigment and more recently in various catalytic applications such as NO_x reduction[10,11] and Fischer−Tropsch synthesis.[12,13] Despite the interest generated, many aspects regarding geometric and electronic structure of both the bulk and the surfaces are not well-understood or even unknown. At room temperature, $CoAl_2O_4$ is an almost normal spinel[14] (i.e., most of Co^{2+} ions are situated at the tetrahedral sites and most Al^{3+} ions occupy octahedral sites in the slightly distorted cubic close packed oxygen sublattice). At high temperatures, part of the Co^{2+} and the Al^{3+} ions may interchange their positions. The temperature dependence of the cation distribution in $CoAl_2O_4$ has been studied from X-ray experiments on quenched samples[14−16] and from in situ optical transmission measurements.[17,18] The main result is that the degree of inversion

* To whom correspondence should be addressed. Phone: 33-1-44-27-96-60; fax: 33-1-44-27-41-17; e-mail: tielens@lct.jussieu.fr.
† Université Pierre et Marie Curie.
‡ Universidad de Oviedo.
§ ICREA and ICIQ.

10.1021/jp053375l CCC: $33.50
Published on Web 12/17/2005

increases smoothly at higher temperatures although a considerable scatter in the data is found. This lack of reproducibility can be attributed to the fast reequilibration kinetics of the cation distribution in quenched samples.[18] Neutron spectroscopy experiments on the same system determined the crystal field transitions.[19]

Theoretical ab initio studies on AB_2O_4 spinels used to concentrate on their structural and electronic properties or on pressure-induced phase transitions and decompositions into the simpler oxides AO_2 and B_2O_3 (see, for example, refs 20−22 and references therein). More recently, combined DFT and Monte Carlo studies have focused on the cation distributions in spinels.[23,24] However, to the best of our knowledge, no previous works have dealt with the $CoAl_2O_4$ spinel yet. Modeling structures with variable cation distributions is becoming nowadays feasible using static, total energy first-principles computational tools. These methods can contribute to the understanding of the global behavior exhibited by known (observed) and new (expected) $(Co_{1-x}\ Al_x)[Co_xAl_{2-x}]O_4$ spinels in terms of local and microscopic properties derived from quantum-mechanical calculations.

Here, we present the first theoretical work dedicated to the structural and electronic properties of bulk $(Co_{1-x}Al_x)[Co_xAl_{2-x}]O_4$ spinels. Explicitly, supercell calculations under the density functional theory (DFT) framework have been performed for $x = 0$, 0.25, 0.33, 0.50, 0.66, 0.75, and 1. Special attention has been given to the cation distribution by means of the evaluation of the dependence of the degree of inversion parameter on temperature. Details of the crystal modeling and of the computational methods are given in the Computational Details. The presentation and discussion of the results are organized in three subsections. The first one provides static (zero-temperature and zero-point vibrational contributions neglected) total energy values and several equilibrium geometrical parameters of all the spinels considered. The second one includes equations of state isotherms and the analysis of the stability of the spinels with temperature. This section ends with the examination of the optimized spin polarized electronic states of Co^{2+} and their implication on the magnetic behavior of spinels with different degrees of inversion. Finally, the main conclusions are summarized in the last section.

Computational Details

Crystal Modeling. The conventional unit cell of the $CoAl_2O_4$ spinel structure contains eight formula units, and it is cubic and belongs to the *Fd*3*m* space group (227). Cations occupy 8a and 16d special Wyckoff positions of T_d and O_h symmetries, respectively, at (1/8, 1/8, 1/8) and (1/2, 1/2, 1/2), whereas oxygens occupy the 32e general position at (*u*, *u*, *u*), *u* being the positional parameter of oxygen.[25] O^{2-} anions build an almost face-centered cubic matrix, the metal cations being distributed over the octahedral and tetrahedral interstices. In the cation distribution of the normal ($x = 0$) spinel unit cell, eight of the 64 tetrahedral sites and 16 of the 32 octahedral sites are occupied, respectively, by Co^{2+} and Al^{3+}. It should be noted that the spinel is a relatively open structure since only around 33% of the volume of the octahedral and tetrahedral voids is occupied by cations.[22]

Most of the standard solid-state computational packages use the smallest irreducible cell instead of the conventional unit cell to solve the electronic structure of the crystal. The advantage of using this primitive cell is to decrease computational efforts while keeping the physics of the system unaltered. The primitive unit cell of the normal spinel structure consists of a hexagonal

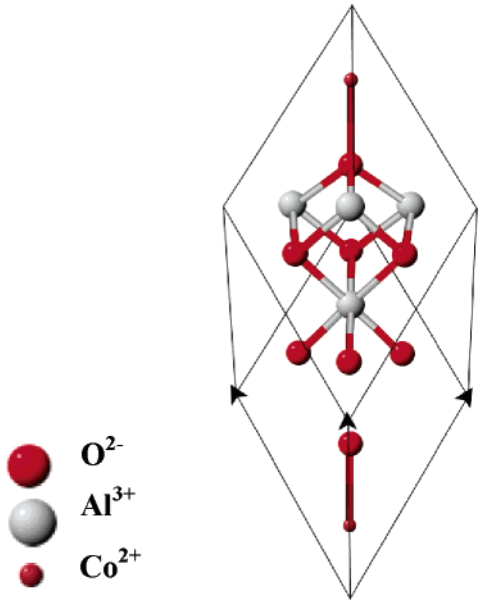

Figure 1. Hexagonal cell used in the calculations.

cell (see Figure 1) with two $CoAl_2O_4$ formula units, 4 times smaller than the conventional cell. This hexagonal cell is also appropriate to describe the spinel structures with $x = 0.5$ and $x = 1$ since it is only necessary to interchange the positions of, respectively, one and two Co^{2+} cations with one and two Al^{3+} cations. In the case of $x = 0.25$ and $x = 0.75$, one-quarter and three-quarters of the Co^{2+} cations, respectively, have to interchange their positions with Al^{3+} cations. Therefore, we need at least four Co^{2+} cations in the unit cell, and a supercell containing four $CoAl_2O_4$ formula units has been used to modelize these spinel structures. Finally, we have also considered spinels with $x = 0.33$ and $x = 0.66$. Here, a supercell of three primitive unit cells of the $x = 0$ spinel is needed to account for the change in the position, respectively, of two and four of the six Co^{2+} cations from the tetrahedral to the octahedral sites (the same number of Al^{3+} ions moves from the octahedral to the tetrahedral sites). In these spinels, the number of formula units in the unit cell is six. Other values of the inversion parameter involve larger cells with at least eight formula units and have not been explicitly considered in this work since the computational time seriously increases with the size of the supercells.

Computational Methods. Every geometry optimization and minimization of the total energy have been performed using the VASP code.[26,27] The energy calculated in VASP is the total energy, including the electron−electron interaction, the electron−nuclei interaction, and the nuclei−nuclei interaction. In the periodic DFT framework used, the Kohn−Sham equations have been solved by means of the generalized gradient approximation (GGA-PW91) proposed by Perdew and Wang.[28,29] The electron−ion interaction was described by the Projector Augmented-Wave method (PAW).[30,31] The plane-wave expansion was truncated at a cutoff energy of 400 eV. For the Brillouin-zone integration, a $6 \times 6 \times 6$ Monkhorst−Pack special *k*-points grid has been used; the number of *k*-points has been adjusted to the size of the supercell considered to keep the same number of *k*-points in the reciprocal space. We carefully checked the convergence of the energy with respect to the *k*-points. A spin-unrestricted approach has been employed, and the spin state has been optimized. A full optimization of atom positions, cell shape, and volume has been performed via the action of a conjugate gradient optimization procedure.

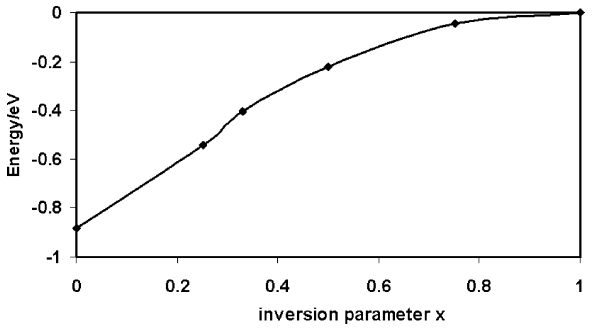

Figure 2. Calculated total energies of the $CoAl_2O_4$ spinels at static conditions for $x = 0$, 0.25, 0.33, 0.50, 0.75, and 1.

As a result of our VASP calculations, sets of energy-volume values (E_i, V_i) for the different spinels considered were obtained. Each of these sets has been carefully described by means of numerical and analytical equations of state implemented in the GIBBS program, described elsewhere.[32,33] This fitting procedure provides the bulk modulus, and its first pressure derivative was evaluated at zero pressure, B_0 and $B_{0'}$, respectively, for all the spinels considered. In particular, the values reported here for these parameters come from the Vinet EOS[34]

$$\ln H = \ln B_0 + A(1-y);\ H = py^2/(3(1-y));\quad A = 3(B_{0'}-1)/2;\ y = (V/V_0)^{1/3} \quad (2)$$

where V and V_0 are the volumes per formula unit at pressure p and at $p = 0$, respectively. The inclusion of thermal effects is performed by means of a nonempirical quasi-harmonic Debye-like model.[32,35] This model is a simple and useful theoretical tool for the calculation of thermodynamic properties of crystals at finite temperatures. The model follows an isentropic approximation that allows the evaluation of Debye temperatures at different volumes from the adiabatic bulk modulus

$$\Theta_D(\mathrm{V}) = \mathrm{h}/(2\pi k_\mathrm{B})[6\pi^2 V^{1/3} r]^{1/3}[B_\mathrm{S}/\mathrm{M}]^{1/2} f(\sigma) \quad (3)$$

where h is Planck's constant, k_B is the Boltzmann constant, M is the molecular mass, r is the number of atoms in the unit formula ($r = 7$ in $CoAl_2O_4$), B_S is the adiabatic bulk modulus of the crystal, and σ is the Poisson ratio. This property is crystal dependent and changes with T and p. To avoid the σ-dependence of Θ_D, we set $\sigma = 0.25$, the value of the Cauchy solid. In the previous equation, B_S depends on V and T. Our Debye-like model reduces Θ_D to be a function of V since B_S is approximated by the static bulk modulus (B_{static}) calculated from the total energy-volume relationship obtained with VASP or with the Vinet EOS

$$B_{static} = V(d^2E/dV^2),\ B_{static} = -1/y^2(B_0 e^{A(1-y)}(y - 2 - Ay(1-y))) \quad (4)$$

Once Θ_D is calculated, the thermodynamic properties (in particular, the vibrational contribution to the internal energy E_{vib} and the vibrational entropy S_{vib}) are evaluated following the well-known equations of the Debye model.[32]

Results and Discussion

Structure and Cation Distribution. Figure 2 plots the total energy at the calculated equilibrium static geometries of all the $CoAl_2O_4$ spinels considered in this work versus the degree of inversion x. According to our static calculations, the most stable structure is found to be the normal spinel structure. It is known that the position of the trivalent cations at octahedral sites in spinels is favored by the Madelung electrostatic field generated by the oxygen sublattice. At the O_h site, it is greater than at the T_d one, and thus, the electrostatic field would stabilize the cation with the largest formal charge in the O_h site. At room temperature, the experimental observations also identify $CoAl_2O_4$ as an almost normal spinel in equilibrium (i.e., $x \approx 0$).[14] Thermal effects up to 300 K are expected to have a low influence in the actual value of x. Although our result is in agreement with the experimental findings, it may be also seen in contradiction with the expected effect of cation size and electronegativity of Co^{2+}. Indeed, the biggest cation should occupy the biggest site, so Co^{2+} should be in the octahedral site ($r_{Al}^{3+} = 0.51$ Å $< r_{Co}^{2+} = 0.72$ Å).[36] Regarding the atomic electronegativity, the most electronegative cation should interact with the least number of anions, so the Al^{3+} ion should occupy the tetrahedral sites ($\chi_{Co} = 1.47 < \chi_{Al} = 1.54$).[37] This point was also raised by Nakatsuka et al.,[15] who explained this behavior using mean Al−O, Co−O, and O−O bond lengths of $CoAl_2O_4$ spinels with different x values. As they could not synthesize a $CoAl_2O_4$ spinel with a degree of inversion higher than 0.23, the extrapolation of the measurements was inevitable to obtain geometrical parameters for higher x values. In the present study, we are not limited by experimental constraints but for the size of the cells needed to achieve a certain value of x. Nevertheless, we could investigate cell models with selected x values covering the whole range between 0 and 1, and therefore, we can complement the information required in the experimental studies.

The static equilibrium configuration of $CoAl_2O_4$ in the normal spinel configuration ($x = 0$) is found at $a = 8.092$ Å and $u = 0.2641$, which is in very good agreement with the experimental values[14] of $a = 8.106$ Å and $u = 0.2631$ for $x = 0.107$ at 850 °C. As discussed next, the lattice parameter shows an almost negligible variation with x according to our calculations. The results for the optimized geometry and bond lengths are summarized in Tables 1 and 2, where they are compared with the experimental ones.

The switch of cobalt ions from tetrahedral to octahedral environment, and the opposite for aluminum, introduces slight geometrical changes in the unit cell volume and greater effects on the oxygen positional parameter. Figure 3 shows that the lattice parameter a decreases (see also Table 1) as x increases up to $x = 0.66$, and then a increases until the inverse configuration is reached. The u parameter decreases gradually until $x = 2/3$ and rapidly beyond this value (see Figure 4). These results are not experimentally available for the complete x range.

Experimentally, the relation between the cation distribution and the lattice parameter a is equivocal. Nakatsuka et al.[15] observed an increase with the degree of inversion, whereas O'Neill[14] concluded that the a parameter of $CoAl_2O_4$ did not change with the cation distribution. Our predictions show a minimum in the cell parameter a for $x = 2/3$; however, the variation in a over the whole x range is 0.08 Å, which is less than 1% (see Figure 3 and Table 1).

The analysis of the Co−O and Al−O bond lengths versus the inversion parameter is shown in Figure 5 and Table 2. The relative deviation of the average M−O distances (M: Co or Al) is at most 3% in the case of a tetrahedral environment and 5% in the case of an octahedral environment. The maximum deviation values are found for $x = 0.50$. Octahedra are more influenced by deformation due to cation redistribution than tetrahedra. Two groups of curves can be distinguished: those decreasing at large x and those showing the opposite trend. The curves converging to a relative similar value are $d(Al-O)O_h$

TABLE 1: Theoretical and Experimental Static Cohesive Properties of Bulk $CoAl_2O_4$ for Different Values of the Inversion Parameter *x*

	0	0.25	0.50	0.75	1	exp. ($x = 0.107$; samples at 750 °C)	exp. ($x = 0.109$; samples at 750 °C)
a/Å	*8.092*	*8.068*	*8.030*	*8.020*	*8.098*	*8.106*[14]	*8.103*[15]
u	0.2641	0.2630	0.2623	0.2600	0.2539	0.2631[14]	0.2639[15]
V/Å^3	66.22	65.50	64.77	64.69	65.23	66.58[14]	66.50[15]
B_0/Gpa	197.3	199.4	196.9	193.8	218.8		
B_0	4.2	4.3	4.2	4.9	3.5		
ΔE^a/kJ mol^{-1}	0.0	15.6	40.1	42.7	37.3		

[a] ΔE being defined as relative to the normal spinel.

TABLE 2: Average Interatomic Distances for Different *x* Values of $CoAl_2O_4$ Structures[a]

coordination		0	0.25	0.50	0.75	1	exp.	0	1
O_h	d(Al−O)	1.916	1.923	1.915	1.918	1.915		1.913[15] 1.915[36]	
O_h	d(Co−O)		1.975	1.997	2.048	2.035			2.057[15] 2.125[36]
T_d	d(Al−O)		1.840	1.837	1.803	1.793			1.836[15] 1.77[36]
T_d	d(Co−O)	1.949	1.948	1.929	1.926			1.962[15] 1.96[36]	
	d(O−O)tetra(Al)		2.979	2.928	2.983				
	d(O−O)tetra (average)							2.999[15]	3.203[15]
	d(O−O)tetra(Co)	3.183	3.193	3.130	3.141				
	d(O−O)sh[b](Al)	2.538	2.538	2.629	2.634	2.652			
	d(O−O)sh (average)							2.526[15]	2.746[15]
	d(O−O)sh(Co)		2.616	2.689	2.698	2.773			
	d(O−O)unsh[b](Al)	2.870	2.834	2.809	2.778	2.801			
	d(O−O)unsh (average)							2.874[15]	2.871[15]
	d(O−O)unsh(Co)		2.960	2.978	2.978	3.013			

[a] Distances in angstroms. [b] unsh: unshared and sh: shared.

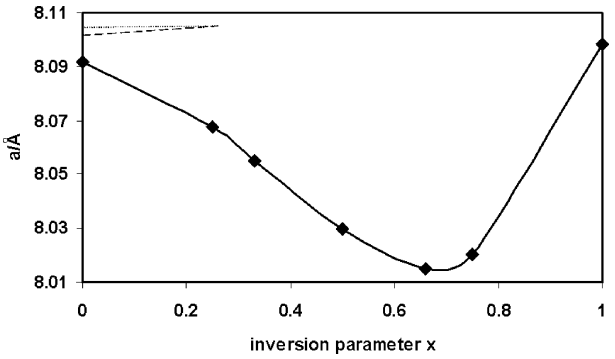

Figure 3. Lattice parameter a (in Å) vs the inversion parameter x (full line: this work; dotted line: ref 14; and dashed line: ref 15).

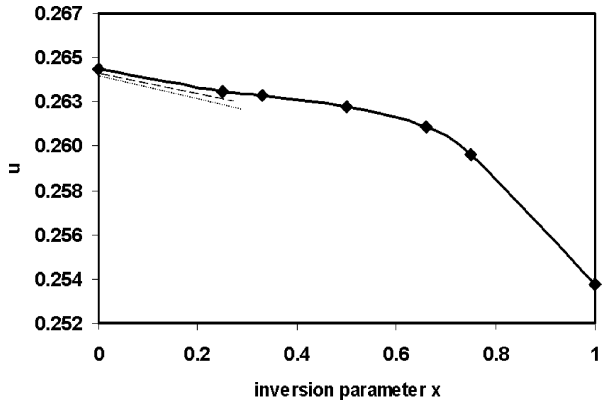

Figure 4. Optimized parameter u vs the inversion parameter x.

and d(Co−O)T_d. Both distances in the normal spinel ($x = 0$) are in agreement with the results of Nakatsuka et al.[15] However, it was found from extrapolation of experimental data[15] that the distances evolve to the same value already at approximately $x = 0.25$, as beyond this value d(Al−O)O_h becomes shorter and

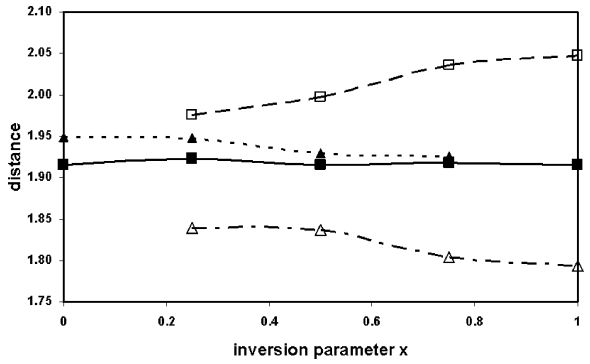

Figure 5. Averaged aluminum and cobalt oxygen distances vs the inversion parameter x (distances in angstroms, ■: dAl−O(O_h), □: dCo−O(O_h), ▲: Co−O(T_d), and △: Al−O(T_d)).

d(Co−O)T_d becomes larger. In our calculations, we can discriminate between a tetrahedron filled with a Co or an Al atom, which is far more difficult to assess experimentally and was not investigated by Nakatsuka et al. Consequently, their curves were mixtures of Al and Co. To be able to compare with the experimental results, the distances d(M−O) (M = Al or Co) were averaged over four and six distances in a tetrahedron and octahedron, respectively. Taking this into consideration, the same trend from the experiment and theory was obtained. However, it should be emphasized that the effect of shrinking and expanding of d(M−O) is mainly caused by d(Al−O)T_d and d(Co−O)O_h.

Concerning the O−O distances (Figure 6 and Table 2), one can distinguish three different types, namely, the tetrahedral, shared, and unshared octahedron in the spinel structure. A decrease of the d(O−O)tetra, an almost constant evolvement of the d(O−O)unshared, and an increase of the d(O−O)shared is observed, which is also in line with the trend observed experimentally. Looking at the separate types (Co and Al), the

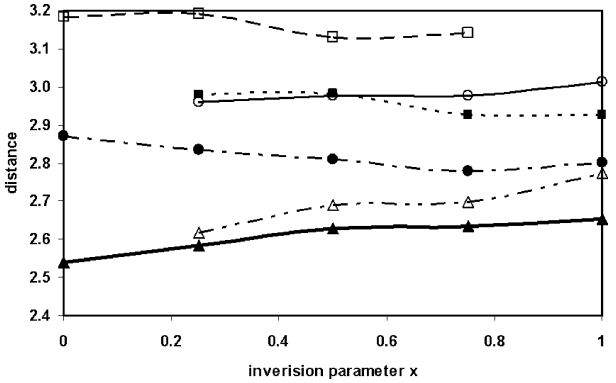

Figure 6. Different averaged oxygen−oxygen distances present in the $CoAl_2O_4$ spinel vs the inversion parameter x (distances in angstroms, ■: d(O−O)tetra(Al), □: d(O−O)tetra(Co), ▲: d(O−O)sh(Al), △: d(O−O)sh(Co), ○: d(O−O)unsh(Al), and ●: d(O−O)unsh(Co)).

trends are the same except for d(O−O)unshared, where cobalt acts oppositely to aluminum. The combination of both gives practically no change versus x.

These geometrical results suggest that the substitution of Co^{2+} in tetrahedral sites introduces a great perturbation that would not be energetically favorable. The enlargement of the d(Co−O)T_d site with increasing x is recovered; however, the d(Co−O)T_d distance of 2.057 Å obtained after extrapolation for a hypothetic $x = 2$ (complete Co spinel considered in ref 13) is slightly overestimated (2.048 Å). This finding is investigated more in detail considering the electronic structure of the system, as is discussed in the next sections.

Pressure and Temperature Effects on the Spinel Structure. On the basis of a previous systematic study of 149 oxide and 80 sulfide binary and ternary spinels,[2] Finger et al.[38] suggested that all oxide spinels may have a similar bulk modulus around 200 GPa. For example, values of 196, 197, 198, and 206 GPa have been reported for $MgAl_2O_4$, $ZnMn_2O_4$, $CuMn_2O_4$, and $NiMn_2O_4$ (see ref 39). The behavior of $CoAl_2O_4$ under hydrostatic pressure (see Table 1) follows this result with B_0 values for the spinels of different inversion parameters in the range from 193.8 to 218.8 GPa. Theoretical studies have identified the oxygen sublattice of AB_2O_4 spinels as mainly responsible for this uniform behavior. Oxygen atoms occupy more than 70% of the unit cell space and compress almost at the same rate as the crystal does.[40] An alternative interpretation based on the constitutive polyhedra of normal spinels (AO_4 and BO_6) found that the average of the tetrahedral and octahedral compressibilities is a very good estimation of the bulk compressibility. This study also identified tetrahedra occupied by divalent cations as the more compressible units when pressure is applied.[41] However, if the tetrahedra are occupied by a trivalent cation, the corresponding polyhedral compressibility decreases below the crystal compressibility. On the other hand, octahedra occupied by divalent cations are easier to compress than octahedra occupied by a trivalent cation. In $CoAl_2O_4$, this analysis indicates that it is the balance between the increase in compressibility when Co^{2+} goes to the octahedral sites and the decrease in compressibility when Al^{3+} goes to the tetrahedral sites that determines the actual values of B_0 of spinels with different degrees of inversion.

In spinels with cation distributions other than in the normal structure, the compressibility is not a simple average of two polyhedral compressibilities since up to four polyhedra are involved (AO_4, AO_6, BO_4, and BO_6), and a continuous trend of the bulk compressibility with the inversion parameter from $x = 0$ to 1 is not to be expected. In $CoAl_2O_4$, we find that all

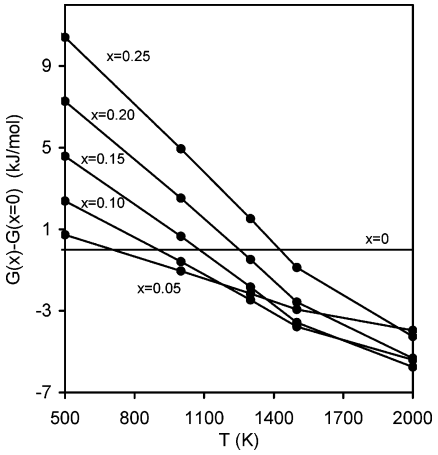

Figure 7. Temperature dependence of the relative stability of $CoAl_2O_4$ spinels with different x values. Gibbs energies are referred to the $x = 0$ spinel.

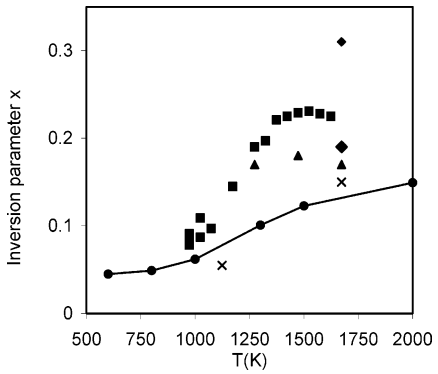

Figure 8. Variation of the inversion parameter (x) with temperature. Symbols stand for the experimental data: ■,[15] ▲,[43] ◆,[44] and ×,[45] whereas the solid curve contains our calculated values (●).

spinels with $x \neq 1$ have a bulk modulus close to 198 GPa, whereas the value in the inverse spinel is around 10% higher. A similar result has been obtained in other oxide spinels as $MgGa_2O_4$.[41] It seems that in the special case of the inverse spinel, the fact that all the tetrahedra are occupied by trivalent cations dominates the response of the structure to pressure yielding to a strong effect in the reduction of the bulk compressibility.

The thermal effects over the electronic energy can be decoupled in two contributions: vibrational internal energy (E_{vib}) and vibrational entropy (S_{vib}), both evaluated with the GIBBS code. Moreover, we have to include an entropic term associated with the different configurations available for a given degree of inversion x:[42]

$$S_{conf} = -R[x\ ln\ x + (1-x)ln(1-x) + x\ ln\ x/2 + (2-x)ln(2-x)] \quad (5)$$

Because of the smooth and continuous variation of E, E_{vib}, S_{vib}, and S_{conf} with V, T, and x, we have carried out interpolations to compute with a reasonable precision the total Gibbs energy (G) using the following expression:

$$G = E + E_{vib} - TS_{vib} - TS_{conf} \quad (6)$$

The interpolations cover the range of inversion parameters with experimental information[15,43−45] (i.e., from $x = 0$ to $x \approx 0.25$).

These results are showed in Figures 7−9. Our first interesting finding is that the calculations are able to describe the change in stability of $CoAl_2O_4$ spinels with different degrees of

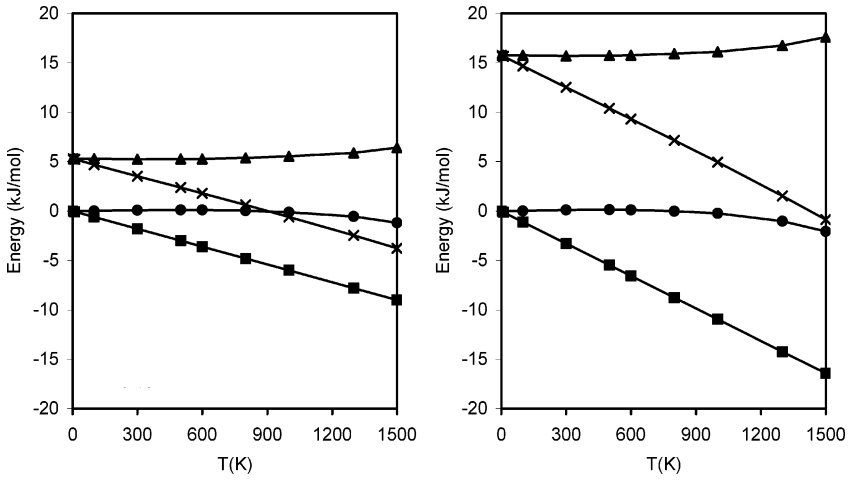

Figure 9. Temperature effects on ΔG (crosses), ΔE (triangles), $-T\Delta S_{vib}$ (circles), and $-T\Delta S_{conf}$ (squares) for $x = 0.10$ and $x = 0.25$.

inversion as the temperature increases. The evaluation of G for spinels with $x = 0$, 0.05, 0.10, 0.15, 0.20, and 0.25 shows that the inversion parameter associated with the lowest value of G increases with the rise of temperature in the range from 500 to 2000 K (see Figure 7). This result supports our simplified supercell models used in the computational simulation since a good qualitative agreement with the observed data was found. Experimental values show slightly greater inversion degrees (never more than $x = 0.31$, most of them between 0 and 0.25) and exhibit the same general trend as the one obtained in our calculation (see Figure 8). We can confirm that it is highly unlikely to synthesize $CoAl_2O_4$ with $x > 0.3$, even at very high temperatures. Probably, the lack of an explicit temperature-dependent electronic term (electronic entropy) and the reduced size of our supercell models are the two main reasons to explain the discrepancy with respect to the experimental $x - T$ data. A more accurate evaluation of the vibrational entropy may also introduce some corrections in our results, although we have checked (not in $CoAl_2O_4$, but in other oxides as $ZrSiO_4$) that most of the thermodynamic properties evaluated with our Debye-like model are in good agreement with the values calculated with a more sophisticated quasi-harmonic model involving explicit calculation of vibrational frequencies at the Γ-point.

The analysis of the different energetic contributions to G depicted in Figure 8 shows that the component that involves the configurational entropy ($-T\Delta S_{conf}$) is the one that causes the stabilization of the spinels with $x \neq 0$ as temperature is increased. Our calculations show that, although TS_{vib} obviously increases with T and is quite larger than TS_{conf} (TS_{vib} is 290 kJ/mol and TS_{conf} is 11 kJ/mol at 1000 K and $x = 0.25$), the vibrational entropy practically has the same value in all the spinels, independent of the x value, and therefore, this term is not important in the stabilization of the spinels with different inversion parameters. On the other hand, as we have pointed out, the electronic energy term disfavors the existence of $x \neq 0$ spinels as x and T increase. This electronic energy contribution is namely responsible for the absence of spinels with greater degrees of inversion (in particular, for $CoAl_2O_4$).

Spin Density. An investigation of the spin states present in the different spinel configurations ($x = 0$ to $x = 1$) has been carried out to elucidate the nature of the magnetic properties of the $CoAl_2O_4$ spinel. Co^{2+} has the electronic configuration s^0d.[7] Since the spinels contain Co^{2+} in different environments, we have analyzed the final spin in terms of the crystal field theory: the splitting of the d orbitals in the octahedral environment stabilizes the t_{2g} with respect to the e_g orbitals,

TABLE 3: Spin Values Obtained for the Different x Values Considered[a]

system	x	spin	no. of Co^{2+} in T_d	no. of Co^{2+} in O_h
$Co_2Al_4O_8$	0	6 (12)	2 (4)	
$Co_4Al_8O_{16}$	0.25	8	3	1
$Co_4Al_8O_{16}$	0.50	4	2	2
$Co_4Al_8O_{16}$	0.75	6	1	3
$Co_2Al_4O_8$	1	6 (12)	0	2 (4)
Co_3O_4		6 (12)	2 (4)	2 (4) Co^{3+}

[a] In parentheses normalized to $Co_4Al_8O_{16}$ for comparison.

while the tetrahedral coordination leads to a stabilization of the e orbitals with respect to t_2. The electron distribution depends on the strength of the crystal field, so high spin (weak field) and low spin (strong field) states are possible.[5] Table 3 contains the spin values for the spinels considered (note that the results are normalized to four $CoAl_2O_4$ formulas). Because of computer limitations, spinels with $x = 0.33$ and 0.66 were not investigated. During geometry optimization, the spin state was optimized. No influence of the cell size or symmetry has been found in the spin distribution for $x = 0$, 0.5, and 1. The Co_3O_4 and Al_3O_4 spinel structures have also been considered for comparison.

For the normal $CoAl_2O_4$ ($x = 0$) spinel structure containing only tetrahedral Co^{2+}, three unpaired electrons are found per Co^{2+} ion (a spin state of 12 for a $Co_4Al_8O_{16}$ formula). The e orbitals are completely filled, and the t_2 orbitals are replenished by the unpaired electrons as schematically shown in Figure 10. This corresponds to a typical high spin (weak field) configuration for a tetrahedral system. The inverse spinel possesses all the Co^{2+} ions in octahedral coordination, and the electrons fill t_{2g} and e_g again as for a high spin (weak field) configuration leading to a final spin state of 12 for a $Co_4Al_8O_{16}$ formula.

For $x = 0.25$, there are three tetrahedral and one octahedral Co^{2+} in the $Co_4Al_8O_{16}$ unit cell, and 10 unpaired electrons are found leading to a final spin state of eight. In this case, spin down electrons come into play indicating antiferrimagnetic properties of the material. The electronic distribution according to our calculation is as follows: each tetrahedral Co^{2+} ion contains three unpaired electrons that occupy the t_2 orbitals, and this is nine electrons; the octahedral Co^{2+} ion e_g orbital is filled with one β electron. Note that the octahedral configuration in this case corresponds to a low spin (strong field). The same explanation is applied to the spinel with $x = 0.5$, resulting in eight unpaired electrons and a final spin state of four: two high spin tetrahedral Co^{2+} ions and two low spin octahedral Co^{2+} ions filled with unpaired β electrons lead to the calculated spin distribution.

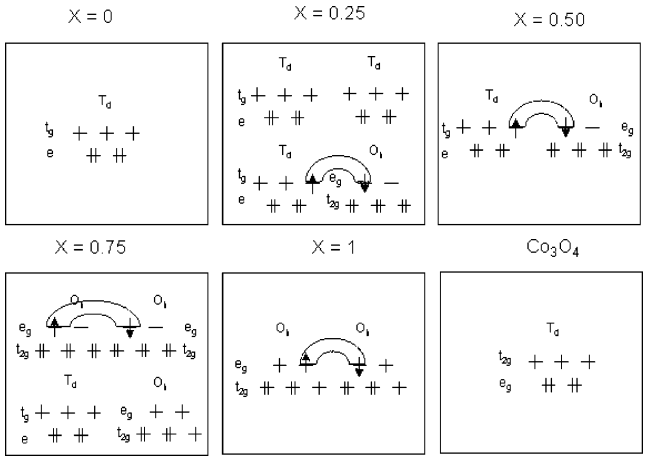

Figure 10. Electronic configuration for the Co^{2+} ions in T_d and O_h coordination in $CoAl_2O_4$ for different values of *x*. All the tetrahedral sites are high spin (weak field), and all octahedra but one in $x = 0.75$ are low spin (strong field).

The spinel with $x = 0.75$ presents a more complex electronic diagram. The spin optimization results in eight unpaired electrons with a total spin of six. The distribution is as follows: one high spin tetrahedral Co^{2+} ion, two octahedral low spin Co^{2+} ions with each one an unpaired e_g electron (one α and one β), and one high spin (weak field) octahedral ion with three unpaired α electrons according to our results.

In the case of the Co_3O_4 spinel, the same configuration as for $x = 1$ (three unpaired electrons per Co^{2+}) was found. The Al_3O_4 structure was found to be a singlet as expected.

The analysis of the results show that the tetrahedral Co^{2+} ions always present the same spin configuration state, while in the octahedral coordination, both high spin and low spin configurations are found. Indeed, it is seen that high spin states are preferred for *x* values up to 0.5 and low spin configurations for $x > 0.75$. In the special case of $x = 0.75$, we found two different types of O_h Co^{2+}, one with a larger distortion of the Co−O distance than the other (this cannot be immediately seen from Table 3 since only the average value are presented). This distortion is in line with the results of the spin density, where also two different spin configurations are found (high and low spin) for the $Co^{2+}O_h$.

The reason for this behavior is the distortion of the octahedral sites: since the Co−O distances increase, the electrostatic field becomes weaker, and the high spin configurations are stabilized. In other words, the distortion around the octahedra results in a lifting of the degeneracy of the d orbitals. The corresponding energetic levels are closer, and the material becomes conducting. This is also observed from an analysis of the Density of States (not presented), where the band gap decreases when increasing *x*. We conclude that octahedral Co^{2+} is responsible for the variations of magnetic properties in these spinel structures. It is interesting to note that for the intermediate *x* values of 0.25, 0.50, and 0.75, β electrons come into play proving the antiferrimagneticity of the material. The presence of such β electrons was necessary to explain the optimized spin state and would point to the observed magnetism observed in cobalt spinels.

Conclusions

In this study, the $CoAl_2O_4$ spinel was investigated for the first time by means of quantum chemical calculation tools. The periodic DFT calculations predict the normal spinel structure ($x = 0$) to be the most stable in agreement with the experiment. The influence of *x* over its whole range (0−1) is studied on the geometry and electronic/magnetic properties of $CoAl_2O_4$.

Regarding geometry, the lattice parameter of the spinel decreases with *x* until a minimum value for $x = 2/3$, and then it increases beyond this point. However, the variation of *a* over the whole range is less than 1%. The internal parameter *u* smoothly decreases until $x = 2/3$, and beyond this point it drops down. Important geometrical distortions are observed as the Co^{2+} ions occupy octahedral sites that may be the reason for an energetically unfavorable process of substitution.

The compressibility of $CoAl_2O_4$ spinels is similar to other oxide spinel-type compounds with bulk moduli around 200 GPa. Temperature affects the relative stability of $CoAl_2O_4$ with different cation distributions. We account for this phenomenon by coupling a quasiharmonic Debye model to our DFT calculations. As a result, we are able to determine the preference of cation distributions with larger *x* values as the temperature increases, the $x - T$ results following an asymptotic trend. The analysis of the different energetic contribution to the Gibbs energy identifies the configurational entropy component as mainly responsible for the stabilization of the spinels with $x \neq 0$.

The study of the electronic structure reveals interesting features. Whereas tetrahedral Co^{2+} ions always present the same spin state (three unpaired electrons per ion), octahedral Co^{2+} ions pass from a low spin to a high spin configuration as *x* increases (one and three unpaired electrons per ion, respectively). This is the result of the geometrical distortion that increases the Co−O distance and then decreases the crystal field with *x*; as a consequence, a lifting of degeneracy is observed for the d orbitals, and the system becomes conducting. A fine analysis of the electronic structure shows that â electrons are necessary to explain the optimized spin distribution. This could count for the antiferrimagnetic behavior of the cobalt spinels. We conclude that the variations of electronic/magnetic properties are dominated by the octahedral Co^{2+}, which are as intuitively expected in an unsuited environment for a large degree of inversion.

Acknowledgment. R.F. and J.M.R. acknowledge the financial support of the Spanish DGICyT under Project BQU2003-06553. Part of this work was performed under the Project HPC-EUROPA (RII3-CT-2003-506079), with the support of the EU-Research Infrastructure Action under the FP6 "Structuring the European Research Area" Program. Computational facilities provided by IDRIS and CCR are also acknowledged.

References and Notes

(1) Cox, P. A. *Transition Metal Oxides*; Oxford University: Oxford, 1992.

(2) Hill, R. J.; Craig, J. R.; Gibbs, G. V. *Phys. Chem. Mineral.* **1979**, *4*, 317.

(3) Sun, S. H.; Zeng, H.; Robinson, D. B.; Raoux, S.; Rice, P. M.; Wang, S. X.; Li, G. X. *J. Am. Chem. Soc.* **2004**, *126*, 273.

(4) Gabal, M. A.; Ata-Allah, S. S. *Mater. Chem. Phys.* **2004**, *85*, 104.

(5) Bersuker, I. B. *Electronic structure and properties of transition metal compounds*; John Wiley & Sons: New York, 1996.

(6) Burns, R. *Mineralogical applications of crystal field theory*; Cambridge University Press: Cambridge, 1993; Vol. 5.

(7) Borg, R. J.; Dienes, G. J. *The physical chemistry of solids*; Academic Press: San Diego, 1992.

(8) Van Meerssche, M.; Feneau-Dupont, J. *Introduction à la cristallographie et à la chimie structurale*; Peeters: Leuven, Belgium, 1984.

(9) Millard, R. L.; Peterson, R. C.; Hunter, B. K. *Am. Mineral.* **1992**, *77*, 44.

(10) Liotta, L. F.; Pantaleo, G.; Di Carlo, G.; Marcì, G.; Deganello, G. *Appl. Catal., B* **2004**, *52*, 1.

(11) Yan, J.; Kung, M. C.; Sachtler, W. M. H.; Kung, H. H. *J. Catal.* **1997**, *172*, 178.

(12) Voss, M.; Borgmann, D.; Wedler, G. *J. Catal.* **2002**, *212*, 10.

(13) Jongsomjit, B.; Panpranot, J.; Goodwin, G., Jr. *J. Catal.* **2001**, *204*, 98.
(14) O'Neill, H. S. C. *Eur. J. Mineral.* **1994**, *6*, 603.
(15) Nakatsuka, A.; Ikeda, Y.; Yamasaki, Y.; Nakayama, N.; Mizato, T. *Solid State Comm.* **2003**, *128*, 85.
(16) Porta, P.; Anichi, A. *J. Chem. Soc., Faraday Trans. 1* **1980**, *76*, 2448.
(17) He, T.; Becker, K. D. *Solid State Ionics* **1997**, *101*−*103*, 337.
(18) Becker, K. D.; Rau, F. *Solid State Ionics* **1988**, *28*−*30*, 1290.
(19) Winkler, B.; Harris, M. J.; Eccleston, R. S.; Knorr, K.; Hennion, B. *Phys. Chem. Miner.* **1997**, *25*, 79.
(20) Catti, M.; Valerio, G.; Dovesi, R.; Causà, M. *Phys. Rev. B* **1994**, *49*, 14179.
(21) Catti, M.; Freyria-Fava, F.; Zicovich, C.; Dovesi, R. *Phys. Chem. Miner.* **1999**, *26*, 389.
(22) Gracia, L.; Beltran, A.; Andrés, J.; Franco, R.; Recio, J. M. *Phys. Rev. B* **2002**, *66*, 224114.
(23) Lavrentiev, M. Y.; Purton, J. A.; Allan, N. L. *Am. Mineral.* **2003**, *88*, 1522.
(24) Warren, M. C.; Dove, M. T.; Redfern, S. A. T. *J. Phys.*—*Condens. Matter* **2000**, *12*, L43.
(25) Wyckoff, R. *Crystal structures*, 2nd ed.; Wiley-Interscience: New York, 1964.
(26) Kresse, G.; Furthmuller, J. *Comput. Mater. Sci.* **1996**, *6*, 15.
(27) Kresse, G.; Hafner, J. *Phys. Rev. B* **1994**, *49*, 14251.
(28) Perdew, J. P.; Chevary, J. A.; Vosko, S. H.; Jackson, K. A.; Penderson, M. R.; Singh, D. J.; Fiolhais, C. *Phys. Rev. B* **1992**, *46*, 6671.
(29) Perdew, J. P.; Wang, Y. *Phys. Rev. B* **1992**, *45*, 13244.
(30) Blöchl, P. E. *Phys. Rev. B* **1994**, *50*, 17953.
(31) Kresse, G.; Joubert, J. *Phys. Rev. B* **1999**, *59*, 1758.
(32) Blanco, M. A.; Francisco, E.; Luaña, V. *Comput. Phys. Comun.* **2004**, *158*, 57.
(33) Blanco, M. A.; Martín Pendás, A.; Francisco, E.; Recio, J. M.; Franco, R. *J. Mol. Struct. (THEOCHEM)* **1996**, *368*, 245.
(34) Vinet, P.; Rose, J. H.; Ferrante, J.; Smith, J. R. *J. Phys. Condens. Matter* **1989**, *1*, 1941.
(35) Francisco, E.; Recio, J. M.; Blanco, M. A.; Martín Pendás, A.; Costales, A. *J. Chem. Phys. A* **1998**, *102*, 1595.
(36) Shannon, R. D. *Acta Crystallogr., Sect. A* **1976**, *32*, 751.
(37) Sanderson, R. T. *Inorganic Chemistry*; Van Nostrand-Reinhold: New York, 1967.
(38) Finger, L. W.; Hazen, R. M.; Hofmeister, A. *Phys. Chem. Mineral.* **1986**, *13*, 215.
(39) Gerward, L.; Jiang, J. Z.; Staun Olsen, J.; Recio, J. M.; Waskowska, A. *J. Alloys Compd.* **2005**, *401*, 11.
(40) Martín Pendás, A.; Costales, A.; Blanco, M. A.; Recio, J. M.; Luaña, V. *Phys. Rev. B* **2000**, *62*, 13970.
(41) Recio, J. M.; Franco, R.; Martín Pendás, A.; Blanco, M. A.; Pueyo, L. *Phys. Rev. B* **2001**, *63*, 184101.
(42) Navrotsky, A.; Kleppa, O. J. *J. Inorg. Nucl. Chem.* **1967**, *29*, 2701.
(43) Furuhashi, H.; Inagaki, M.; Naka, S. *J. Inorg. Nucl. Chem.* **1973**, *35*, 3009.
(44) Greenwals, S.; Pickart, S. J.; Gannis, F. H. *J. Chem. Phys.* **1954**, *22*, 1957.
(45) Schmalzried, H. *Z. Phys. Chem.* **1961**, *28*, 203.